

PLANT SCIENCE

RALF peptide signaling controls the polytubey block in *Arabidopsis*

Sheng Zhong^{1†}, Ling Li^{1†}, Zhijuan Wang^{1†}, Zengxiang Ge^{1†}, Qiyun Li^{1†}, Andrea Bleckmann², Jizong Wang¹, Zihan Song¹, Yihao Shi¹, Tianxu Liu¹, Luhan Li¹, Huabin Zhou³, Yanyan Wang³, Li Zhang¹, Hen-Ming Wu⁴, Luhua Lai³, Hongya Gu^{1,5}, Juan Dong⁶, Alice Y. Cheung⁴, Thomas Dresselhaus², Li-Jia Qu^{1,5*}

Fertilization of an egg by multiple sperm (polyspermy) leads to lethal genome imbalance and chromosome segregation defects. In *Arabidopsis thaliana*, the block to polyspermy is facilitated by a mechanism that prevents polytubey (the arrival of multiple pollen tubes to one ovule). We show here that FERONIA, ANJEA, and HERCULES RECEPTOR KINASE 1 receptor-like kinases located at the septum interact with pollen tube-specific RALF6, 7, 16, 36, and 37 peptide ligands to establish this polytubey block. The same combination of RALF (rapid alkalization factor) peptides and receptor complexes controls pollen tube reception and rupture inside the targeted ovule. Pollen tube rupture releases the polytubey block at the septum, which allows the emergence of secondary pollen tubes upon fertilization failure. Thus, orchestrated steps in the fertilization process in *Arabidopsis* are coordinated by the same signaling components to guarantee and optimize reproductive success.

Seed plants rely on tightly regulated fertilization mechanisms to secure fertility and reproductive success. Like in animals, the entrance of supernumerary sperm into a single egg—i.e., polyspermy—is restricted to ensure chromosomal balance and progeny health (1, 2). Fertilization in angiosperms is more complex because two sperm cells are carried by one pollen tube that grows in the maternal pistil tissues and ultimately releases its sperm cell cargo inside the ovule (3). Although hundreds of pollen tubes may grow into the transmitting tract of a pistil, usually only a single tube, in response to attractants, emerges from the septum in the vicinity of each ovule to target the ovule (Fig. 1A) (4). The block to polytubey (i.e., the emergence of multiple pollen tubes targeting an ovule) prevents the occurrence of polyspermy. This polytubey block is likely further reinforced by successful gamete fusion that triggers programmed cell death (PCD) of the persistent synergid cell, which leads to the elimination of pollen tube attractants. Thus, the first pollen

tube that emerges from the septum will have the privilege of fertilizing the female gametes, providing a precondition for conspecific pollen precedence (i.e., the preferential use of pollen from the same species for fertilization) (5). If the first pollen tube fails, however, fertilization success will be ensured by fertilization recovery (6, 7), in which the polytubey block is suspended to allow the emergence of secondary pollen tubes for another chance of fertilization. Therefore, plants can (i) restrict polyspermy by enforcing the polytubey block at the septum under normal circumstances and (ii) salvage fertility by removing the polytubey block when fertilization fails. Here, we report the molecular mechanisms by which the polytubey block is implemented or suspended, when needed.

FERONIA, ANJEA, and HERCULES RECEPTOR KINASE 1 receptor kinases are required to establish the polytubey block

To identify factors that may establish the polytubey block, we conducted RNA sequencing (RNA-seq) analysis using transmitting tract and septum tissues and searched for candidate receptors that may perceive signals from the pollen tube. We found that seven malectin-like domain-containing receptor-like kinase (MLD-RLK) (also known as *Catharanthus roseus* RLK1-LIKE or CrRLK1L) genes were highly expressed [verified by real-time quantitative polymerase chain reaction (qPCR); fig. S1, A and B]. Transcriptional and translational markers showed that three of these genes—FERONIA (FER), ANJEA (ANJ), and HERCULES RECEPTOR KINASE 1 (HERK1)—were expressed in the ovule, transmitting tract, and septum epidermis (Fig. 1B and fig. S2). We further realized that a polytubey phenotype can be (i) caused by the failure of establishing the block

at the septum or (ii) triggered by fertilization recovery at the later stage. To distinguish between these polytubey phenotypes, we exploited the *hap2/gcs1* mutant that is defective in gamete fusion and triggers fertilization recovery (8, 9). By CRISPR-Cas9, we obtained the loss-of-function mutant *hap2*−/− (fig. S3) and determined that, when depositing *hap2*−/− pollen on wild-type (WT) pistils, the polytubey phenotype occurs at ~7 hours after pollination (HAP) (Fig. 1, C and D). To determine when the polytubey block occurs at the septum, we observed the growth behavior of WT pollen tubes in semi-in vivo assays (10). It takes a pollen tube 3.5 ± 0.4 hours (*n* = 3 repeats of three to five pollen tubes each) to grow along the funiculus into the ovule and burst (Fig. 1, E and F). Therefore, pollen tubes would emerge in vivo from the septum at ~4 HAP. Accordingly, a polytubey phenotype at the septum should be detectable at 4 HAP in vivo. Thus, we examined the emergence of polytubey at 5, 6, and 7 HAP, contrasting with 12 HAP, that has previously been used for characterizing *fer-4* (11, 12) and/or *anj herk1* mutants (13). Aniline blue staining showed that at 5 to 7 HAP, multiple pollen tubes emerged with comparable growth rates in the receptor mutants *fer-4* (11), *anj herk1*, and *fer anj herk1* (13). This was much more frequent compared with the *hap2*−/− mutant (Fig. 1, C and D, and figs. S4 and S5A). Scanning electron microscopy demonstrated that at 5 HAP, multiple pollen tubes grew at the funiculus of *fer-4*, *anj herk1*, or *fer anj herk1* ovules. This was rarely observed in WT or *hap2*−/− (Fig. 1G). The comparable polytubey ratios of *fer anj herk1* and *fer-4* indicated that FER and/or ANJ and HERK1 receptors may form a receptor complex required for establishing the polytubey block at the septum, which occurs much earlier than the initiation of fertilization recovery in the ovule (6, 7).

Five RALF peptides from pollen tubes trigger the polytubey block

Peptides of the rapid alkalization factor (RALF) family function upstream of MLD-RLK receptors in plant development, immunity response, pollen tube perception, and rupture (12–17). To identify candidate RALF peptides involved in establishing the polytubey block, we examined the pollen-specific MYB transcription factor mutant, *myb97 myb101 myb120*, which showed similar pollen tube reception defects as those observed in *fer-4* and *anj herk1* mutants (18, 19). We found that the emergence of multiple pollen tubes can be observed at 5 to 7 HAP in WT pistils when pollinated by *myb* triple mutant pollen (fig. S6), which indicates the compromised polytubey block at the septum. We thus conducted RNA-seq analysis of *myb* mutant pollen tubes and identified five RALF genes with expression levels

¹State Key Laboratory for Protein and Plant Gene Research, Peking-Tsinghua Center for Life Sciences at College of Life Sciences, Peking University, Beijing 100871, People's Republic of China. ²Cell Biology and Plant Biochemistry, University of Regensburg, 93053 Regensburg, Germany. ³College of Chemistry and Molecular Engineering, Peking University, Beijing 100871, People's Republic of China. ⁴Department of Biochemistry and Molecular Biology, Molecular and Cell Biology Program, Plant Biology Program, University of Massachusetts, Amherst, MA 01003, USA. ⁵The National Plant Gene Research Center (Beijing), Beijing 100101, People's Republic of China. ⁶The Waksman Institute of Microbiology, Rutgers the State University of New Jersey, Piscataway, NJ 08854, USA.

*Corresponding author. Email: qujl@pku.edu.cn

†These authors contributed equally to this work.

‡Present address: Institute of Science and Technology Austria, Klosterneuburg 3400, Austria.

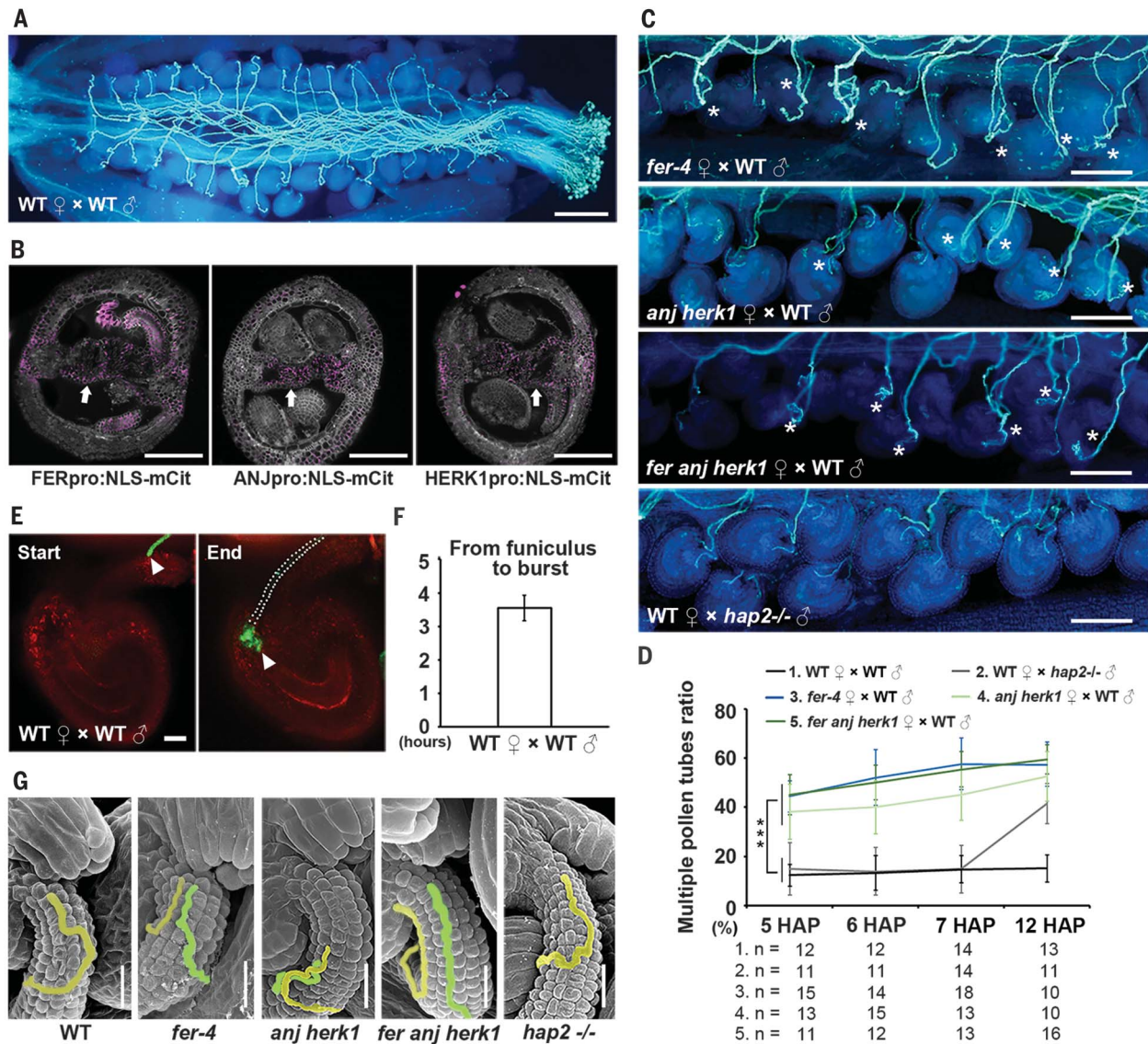


Fig. 1. FER, ANJ, and HERK1 control the polytubey block. (A) A WT pistil pollinated by WT pollen showing that each ovule is targeted by a single pollen tube at 12 HAP. Scale bar, 200 μ m. (B) Cross sections of pistils showing promoter:reporter expression pattern of *FER*, *ANJ*, and *HERK1*. Arrows indicate the septum epidermal layer. Scale bars, 100 μ m. NLS-mCit, mCitrine with nuclear localization sequence. (C) Aniline blue staining showing multiple pollen tubes emerging at the septum at 5 HAP in *fer-4*, *anj herk1*, and *fer anj herk1* pistils pollinated with WT pollen, but rarely in WT pistils pollinated with WT pollen and *hap2*^{-/-} pollen. Asterisks indicate multiple pollen tubes. The analysis was repeated at least three times. Scale bars, 100 μ m.

(D) Statistical analysis of multiple pollen tube ratios, as indicated. “n” refers to the number of pistils. Data are mean values \pm SDs; ****P* < 0.01 (Student’s *t* test). (E) Semi-in vivo assay to determine the duration time of pollen tube growth along the funiculus until rupture in the embryo sac (white arrow heads indicate pollen tubes labeled with LAT52pro:GFP). Dashed dots show position of the pollen tube. Scale bar, 20 μ m. GFP, green fluorescent protein. (F) Statistics of (E). Data are mean values \pm SDs. (G) Scanning electron microscopy images of ovules of WT pistils pollinated with WT pollen and *hap2*^{-/-} pollen and *fer-4*, *anj herk1*, and *fer anj herk1* pistils pollinated with WT pollen at 5 HAP. Scale bars, 20 μ m.

that were lowered or absent in the *myb* triple mutant (fig. S7). They are *RALF6* (At1g60625), *RALF7* (At1g60815), *RALF16* (At2g32835), and two noncanonical *RALF36* (At2g32785) and *RALF37* (At2g32788) (20), which cluster into two subclasses (fig. S7). Their expression in pollen and pollen tubes was further confirmed (Fig. 2, A and B).

Next, we used CRISPR-Cas9 to generate *ralf36 ralf37* double, *ralf6 ralf7 ralf16* triple, and *ralf6 ralf7 ralf16 ralf36 ralf37* quintuple mutants.

They all showed normal vegetative growth behavior (Fig. 2C and figs. S8 and S9). When WT pistils were pollinated with mutant pollen, all three *ralf* mutants showed the polytubey phenotype at 5 to 7 HAP (Fig. 2, D and E, and fig. S5B), resembling what was observed in *fer-4*, *anj herk1*, or *fer anj herk1* mutant pistils pollinated by WT pollen. The higher polytubey ratio caused by *ralf* quintuple than by *ralf* double or triple mutations suggests that the five RALF genes function collectively to estab-

lish a polytubey block. Therefore, we hypothesized that the five RALF peptides are pollen tube-produced signal molecules that are likely perceived by the FER-ANJ-HERK1 receptor complex at the septum to establish a polytubey block.

Because the FER-ANJ-HERK1 receptor complex also controls pollen tube reception at the micropyle (12–14, 21), we next investigated whether the five RALF peptides are also required for pollen tube reception. We observed

that in WT pistils pollinated by *ralf* double and quintuple mutant pollen grains, higher ratios of pollen tube overgrowth (failures in reception) occurred at the micropyle [28.7 ± 7.4% (*n* = 30), 31.1 ± 7.5% (*n* = 30), and 49.2 ±

12.8% (*n* = 22) for *ralf36 ralf37-1*, *ralf36 ralf37-2*, and the *ralf* quintuple mutant, respectively] (Fig. 2, F and G). Consistently, fertility analysis showed that male defects led to obviously reduced fertility in the *ralf* double mutants (70.8 ±

7.8%, *n* = 30, and 68.5 ± 7.7%, *n* = 30, respectively) and more severely in the *ralf* quintuple mutant (57.1 ± 10.9%, *n* = 22, *P* < 0.01 versus *ralf36 ralf37* mutants) (fig. S10). These defects were similar to those observed in *fer-4*, *anj*

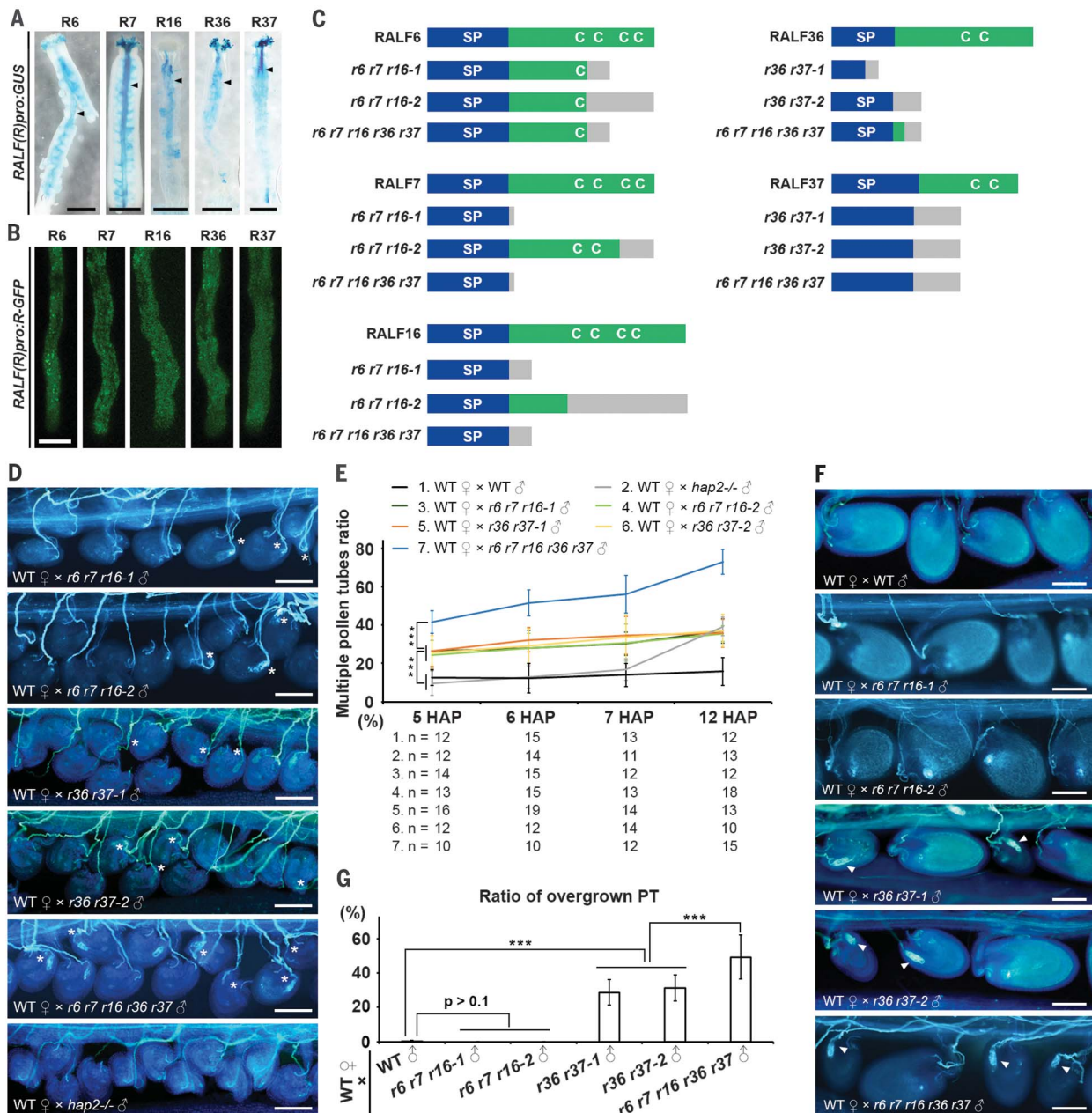


Fig. 2. Pollen-specific RALF6, 7, 16, 36, and 37 peptides control the polytubey block and pollen tube reception. (A) Promoter:GUS plants of five RALF genes show GUS signals in the pollen tubes (black arrowheads). Scale bars, 500 μm. (B) GFP signals in pollen tubes of plants containing RALF-GFP fusion proteins expressed by their native promoter. Scale bar, 10 μm. (C) Schematic diagram of RALF6, 7, 16, 36, and 37 peptide structures showing the positions of conserved cysteine residues and their CRISPR-Cas9-edited mutant structures in *ralf6 ralf7 ralf16* triple (abbreviated as *r6 r7 r16*), *ralf36 ralf37* double (*r36 r37*), and *ralf6 ralf7 ralf16 ralf36 ralf37* quintuple (*r6 r7 r16 r36 r37*) mutants. SP, signal peptide; C, conserved cysteine residue. Gray boxes indicate missense sequences resulting from frame shift mutations. (D) Aniline blue staining

showing multiple pollen tubes emerging at the septum at 5 HAP in WT pistils pollinated with *ralf* triple, double, and quintuple mutant and *hap2-/-* mutant pollen. Asterisks indicate multiple pollen tubes. The analysis was repeated at least three times. Scale bars, 100 μm. (E) Statistical analysis of multiple pollen tube emergence as observed in WT and (D). “n” refers to the number of pistils. (F) Aniline blue staining showing pollen tube overgrowth at the micropyle (white arrowheads) in WT pistils pollinated with WT pollen and *ralf* triple, double, and quintuple mutant pollen at 48 HAP. Arrowheads indicate overgrown pollen tubes. The analysis was repeated at least three times. Scale bars, 100 μm. (G) Statistical analysis of the pollen tube (PT) overgrowth phenotype in pistils shown in (F). Data are mean values ± SDs; ****P* < 0.01 (Student’s *t* test).

herk1, or *fer anj herk1* mutants (fig. S11) (12–14). These findings suggest that RALF6, 7, 16, 36, and 37 are likely the long-pursued ligands of FER and ANJ-HERK1 receptors required for pollen tube reception (12, 13). As both the establishment of a polytubey block at the septum and pollen tube reception in the ovule appear to require the same signaling components, an in-depth mechanistic study on their precisely controlled interaction was necessary.

FER, ANJ, and HERK1 physically interact with RALF6, 7, 16, 36, and 37 peptide ligands

In vitro pull-down assays showed that biotinylated RALF6, 7, 16, 36, and 37 bind to 6×His-tagged ectodomains of FER, ANJ, and HERK1 purified from insect cells or corresponding

maltose-binding protein (MBP)-tagged ectodomains purified from *Escherichia coli* (Fig. 3, A to F). These interactions were strengthened in a peptide dose-dependent manner (Fig. 3, G to I). Microscale thermophoresis (MST) analysis further revealed that both canonical RALF6 and noncanonical RALF36 interact with FER, ANJ, and HERK1 with low equilibrium dissociation constants (K_d) (Fig. 3J), which demonstrates that these RALFs are ligands of FER, ANJ, and HERK1. Moreover, in vitro pull-down assays showed that the addition of RALF6, 36, and 37 promoted the interactions between FER and ANJ-HERK1 receptors (Fig. 3, K and L), which suggests that the RALF6, 36, and 37 peptides may facilitate the formation of larger FER-ANJ-HERK1 heteromeric receptor complexes.

Pollen tube rupture releases the polytubey block and coordinates fertilization recovery

Because the emergence of secondary pollen tubes ensures reproductive success in cases of fertilization failure, the mechanism regulating the polytubey block has to be adjustable. We therefore investigated when and how the polytubey block is removed. After perception by the receptive synergid, the pollen tube bursts to release two sperm cells for double fertilization within ~20 min (4, 22–26). FER-mediated pollen tube reception and production of reactive oxygen species (ROS) in the filiform apparatus region of the ovule have been shown to be required for pollen tube rupture (21). We hypothesized that the presence of RALF peptides is required not only for establishing but also

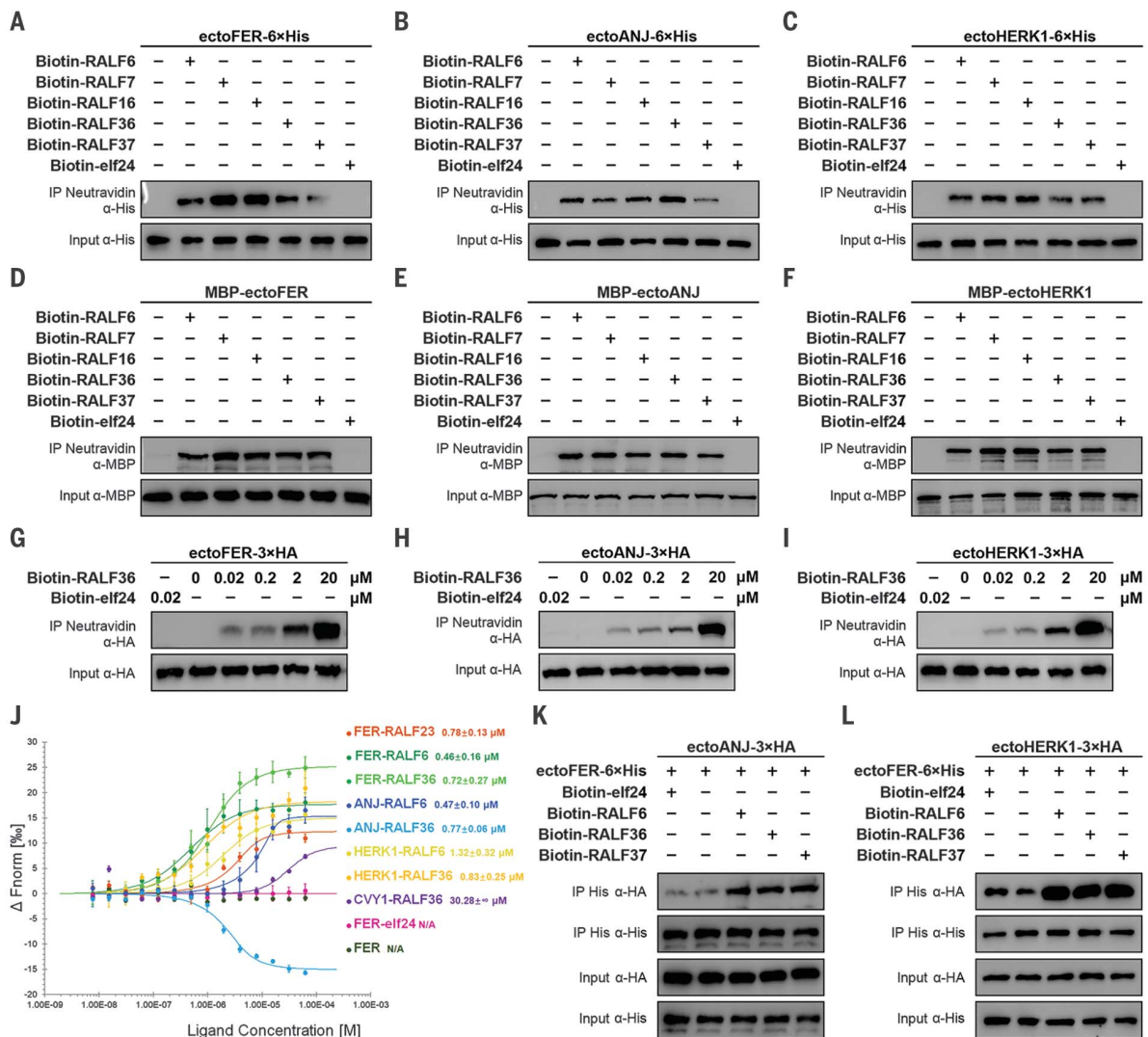


Fig. 3. FER, ANJ, and HERK1 receptors interact with RALF6, 7, 16, 36, and 37 peptide ligands. (A to F) Pull-down assays between 6×His-tagged [(A) to (C)] and MBP-tagged [(D) to (F)] ectodomains of FER, ANJ, and HERK1 and biotinylated RALF6, 7, 16, 36, and 37 and elf24. (G to I) Pull-down assay between HA-tagged FER, ANJ, and HERK1 ectodomains and biotinylated RALF36

obtained by elevating the concentration of RALF36. (J) Binding affinity as indicated by MST analysis. CVY1 and RALF36, FER and elf24, and FER only were used as controls. (K and L) Interaction between 6×His-tagged ectodomains of FER and HA-tagged ectodomains of ANJ and HERK1 by pull-down assays in the presence or absence of RALF6, 36, and 37 peptides.

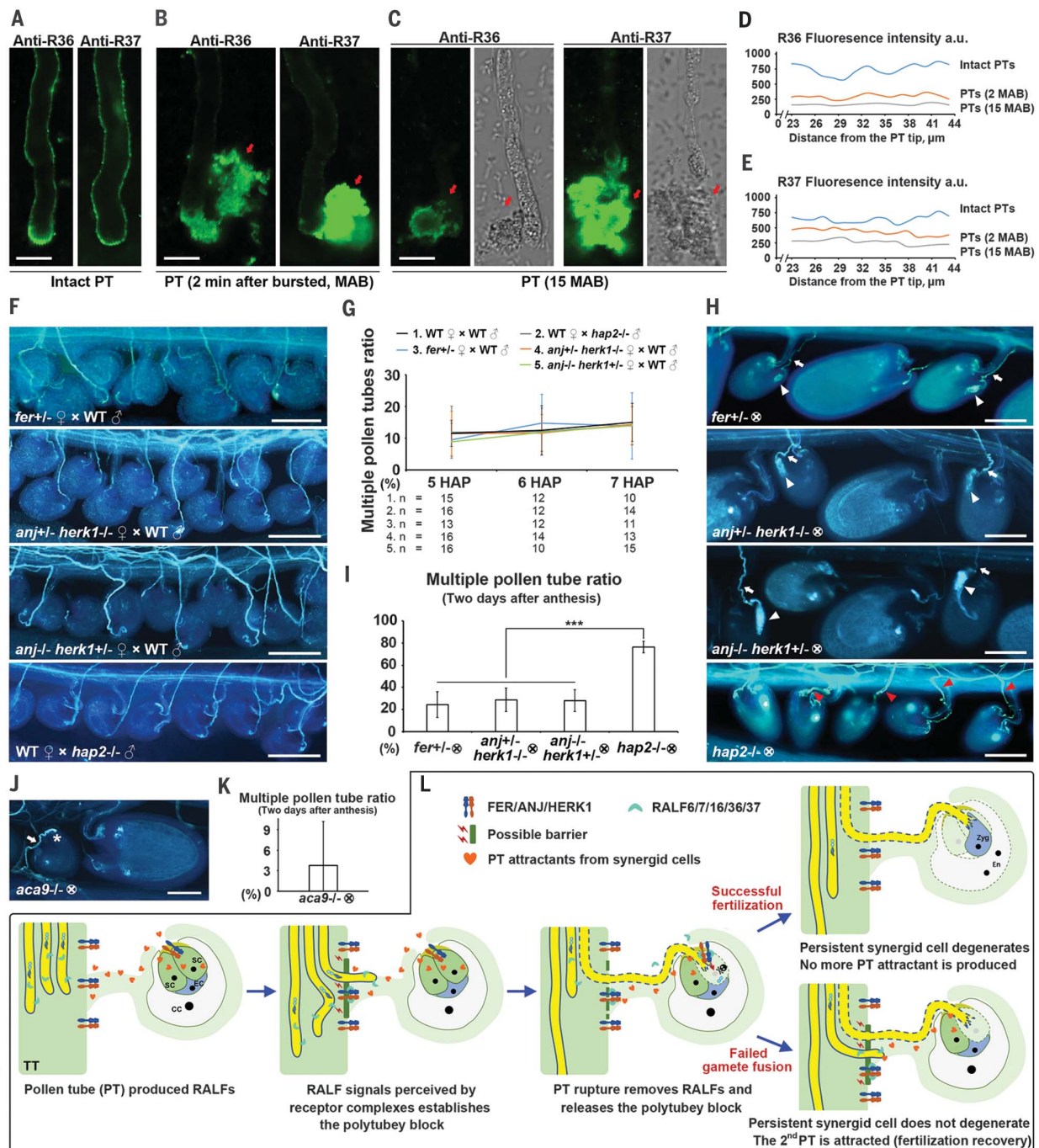


Fig. 4. Pollen tube rupture removes the polytubey block and coordinates fertilization recovery. (A) Immunofluorescence imaging of RALF36 and 37 on the surface of intact pollen tubes. (B and C) Shortly after pollen tube burst (2 min), RALF36- and RALF37-derived fluorescence signal on the pollen tube surface decreased substantially (B) and could scarcely be detected at 15 min (C). Cytosolic RALF36 and 37 (red arrows) were released after pollen tube burst at the tip. The analysis was repeated at least three times. Scale bars, 10 μ m. (D and E) Quantification of immunofluorescence intensity along the shank of the pollen tube surface at stages shown in (A) to (C). Intact pollen tubes and pollen tubes 2 and 15 min after burst (MAB) were measured ($n = 17, 18,$ and 23 for anti-R36, and $n = 22, 20,$ and 18 for anti-R37). a.u., arbitrary units. (F) Aniline blue staining of pollen tube emerging status in *fer+/-*, *anj+/-herk1-/-*, and *anj-/-herk1+/-* pollinated with WT pollen and WT pistil pollinated with *hap2-/-* pollen at 5 HAP. The analysis was repeated at least three times. Scale bars, 100 μ m. (G) Statistical analysis of the multiple pollen tube ratio at

stages indicated in pistils shown in WT and (F). "n" refers to the number of pistils. (H) Aniline blue staining of self-crossed *fer+/-* and *hap2-/-* mutants 2 days after anthesis. White arrowheads indicate overgrown pollen tubes, white arrows mark single pollen tubes in the self-crossed *fer+/-* mutant, and red arrowheads point toward multiple pollen tubes in the self-crossed *hap2-/-* mutant. The analysis was repeated at least three times. Scale bars, 100 μ m. (I) Statistical analysis of multiple pollen tubes ratio in pistils shown in (H). (J) Aniline blue staining of self-crossed *aca9-/-* mutant 2 days after anthesis. White arrow indicates the single pollen tube, and white asterisk indicates blocked pollen tube. Scale bar, 100 μ m. (K) Statistical analysis of multiple pollen tubes ratio in pistils shown in (J). (L) Model of how pollen-specific RALFs act on female tissue located at FER, ANJ, and HERK1 receptor complexes to jointly coordinate establishment, maintenance, and removal of the polytubey block during fertilization progression. TT, transmitting tract; SC, synergid cell; EC, egg cell; CC, central cell; Zyg, zygote; En, endosperm. Data are mean values \pm SDs; *** $P < 0.01$ (Student's t test).

for maintaining the polytubey block at the septum. Thus, pollen tube rupture that naturally terminates the production of RALF peptides would weaken or remove the polytubey block. To test this hypothesis, by using antibodies against RALF36 and 37, we detected immunofluorescence signals in the cell wall of the whole shank region in intact WT pollen tubes but not in the *ralf36 ralf37* mutant (Fig. 4, A, D, and E, and fig. S12). This indicates that the polytubey block can be maintained as long as the pollen tube grows inside the ovule. However, the intensity of RALF36 and 37 signals in the cell wall declined rapidly 2 min after pollen tube rupture (Fig. 4, B, D, and E) and was no longer detectable after 15 min (Fig. 4, C, D, and E), whereas released pollen tube content showed strong immunofluorescence (Fig. 4, B and C). Thus, pollen tube rupture results in the loss of RALF peptides that are required to maintain the polytubey block at the septum and allow secondary pollen tubes to exit the septum.

To genetically test this hypothesis, we examined the receptor mutants *fer+/- (11)*, *anj-/- herk1+/-*, and *anj+/- herk1-/- (13)*. Like WT, these heterozygous mutants should be able to establish and maintain the polytubey block at the septum. Compared with the *hap2-/-* control, none of the three heterozygous mutant pistils exhibited significant emergence of multiple WT pollen tubes at 5 to 7 HAP (Fig. 4, F and G, and fig. S5C). Absence of FER or ANJ-HERK1 in synergids was previously reported to result in failure of pollen tube rupture and impaired fertility, and pollen tube overgrowth can be easily visualized in the mutant ovule (12, 13, 21). We therefore investigated whether selfed heterozygous receptor mutants would show a polytubey phenotype that is triggered by fertilization recovery. Two days after anthesis, in those ovules with failed events of pollen tube rupture (i.e., pollen tube overgrowth), only low levels of polytubey were observed [*fer+/-*, 24.3 ± 11.8% (*n* = 28); *anj-/- herk1+/-*, 28.6 ± 10.5% (*n* = 16); and *anj+/- herk1-/-*, 27.9 ± 9.8% (*n* = 21)], which were much lower than that of the *hap2-/-* mutant (76.4 ± 5.2%, *n* = 12) (Fig. 4, H and I), indicating that the removal of the polytubey block required for fertilization recovery was compromised. We next investigated another mutant, *aca9* [autoinhibited calcium adenosine triphosphatase (ATPase) 9], which showed defects in pollen tube rupture in the ovule (27) (Fig. 4J). Like the receptor mutants, *aca9* did not produce an increased level of polytubey 2 days after anthesis [3.8 ± 6.4% (*n* = 20)] (Fig. 4, J and K). This further confirms that the removal of the polytubey block at the septum depends on pollen tube rupture in the embryo sac. Taken together, the FER, ANJ, and HERK1 receptor complexes not only mediate pollen tube-synergid recognition and subsequent pollen tube rupture in the embryo sac (12, 13), but also function to

trigger the removal of the polytubey block at the septum for fertilization recovery.

Discussion

Here, we have elucidated a molecular mechanism of how FER, ANJ, and HERK1 receptor complexes located at the septum interact with pollen tube-produced RALF6, 7, 16, 36, and 37 peptide ligands to coordinately establish, maintain, and terminate the polytubey block and thus regulate the emergence of pollen tubes to ultimately prevent polyspermy and to ensure reproductive success. On the basis of this and previous studies, we suggest the following model (Fig. 4L): (i) Pollen tube attractants secreted from the synergid cells trigger the nearest pollen tube to exit the transmitting tract. (ii) RALFs secreted from this pollen tube activate FER, ANJ, and HERK1 signaling in septum epidermal cells to establish the polytubey block that prevents the emergence of additional pollen tubes. This male-female jointly established polytubey block remains activated during pollen tube growth into the ovule as a result of the continuous production of RALF peptides by the first-emerged pollen tube. (iii) After successful recognition by the same receptor complex (FER-ANJ-HERK1) in synergid cells, the pollen tube ruptures to release two sperm cells, fertilization will be completed within 20 min (21–26), and the polytubey block is then removed as RALFs quickly disappear from the ruptured pollen tube. (iv) Once fertilization is successful, the persistent synergid cell undergoes fertilization-dependent PCD and fuses with the fertilized central cell. Pollen tube attractants are dispersed, modified, and degraded (11, 28–30), which reduces the attraction of further pollen tubes from the septum despite the release of the polytubey block. Polyspermy is thus prevented. (v) When gamete fusion fails, the persistent synergid cell remains alive and continues to produce pollen tube attractants. Because the polytubey block is removed shortly after pollen tube rupture, secondary pollen tubes are able to emerge from the septum to salvage fertilization. The secondary pollen tube reestablishes the polytubey block, which also explains the low rate of tertiary pollen tubes (6, 23, 30).

This study demonstrates how *Arabidopsis* regulates the emergence of a single pollen tube at the septum to target each ovule and how fertilization success and recovery are interconnected with the activity of the same receptor complexes. It will now be essential to elucidate the downstream mechanism or mechanisms that block the emergence of secondary pollen tubes at the septum. Further components of this polytubey block may include nitric oxide (11); secretion of cell wall components; and ROS that mediate FER-controlled pollen tube rupture (21), pollen hydration (31), and self-incompatibility (32).

REFERENCES AND NOTES

1. D. P. Wolf, *Dev. Biol.* **64**, 1–10 (1978).
2. J. P. Evans, *Mol. Reprod. Dev.* **87**, 341–349 (2020).
3. J. Zhang *et al.*, *Nat. Plants* **3**, 17079 (2017).
4. S. Zhong, L.-J. Qu, *Curr. Opin. Plant Biol.* **51**, 7–14 (2019).
5. S. Zhong *et al.*, *Science* **364**, eaau9564 (2019).
6. K. M. Beale, A. R. Leydon, M. A. Johnson, *Curr. Biol.* **22**, 1090–1094 (2012).
7. R. D. Kasahara *et al.*, *Curr. Biol.* **22**, 1084–1089 (2012).
8. T. Mori, H. Kuroiwa, T. Higashiyama, T. Kuroiwa, *Nat. Cell Biol.* **8**, 64–71 (2006).
9. K. von Besser, A. C. Frank, M. A. Johnson, D. Preuss, *Development* **133**, 4761–4769 (2006).
10. R. Palanivelu, D. Preuss, *BMC Plant Biol.* **6**, 7 (2006).
11. Q. Duan *et al.*, *Nature* **579**, 561–566 (2020).
12. J. M. Escobar-Restrepo *et al.*, *Science* **317**, 656–660 (2007).
13. S. Galindo-Trigo *et al.*, *EMBO Rep.* **21**, e48466 (2020).
14. Z. Ge, T. Dresselhaus, L.-J. Qu, *Trends Plant Sci.* **24**, 978–981 (2019).
15. M. Haruta, G. Sabat, K. Stecker, B. B. Minkoff, M. R. Sussman, *Science* **343**, 408–411 (2014).
16. C. Li *et al.*, *eLife* **4**, e06587 (2015).
17. M. Stegmann *et al.*, *Science* **355**, 287–289 (2017).
18. A. R. Leydon *et al.*, *Curr. Biol.* **23**, 1209–1214 (2013).
19. Y. Liang *et al.*, *PLoS Genet.* **9**, e1003933 (2013).
20. A. Abarca, C. M. Franck, C. Zipfel, *Plant Physiol.* **187**, 996–1010 (2021).
21. Q. Duan *et al.*, *Nat. Commun.* **5**, 3129 (2014).
22. Y. Hamamura *et al.*, *Curr. Biol.* **21**, 497–502 (2011).
23. S. Sprunck *et al.*, *Science* **338**, 1093–1097 (2012).
24. P. Denninger *et al.*, *Nat. Commun.* **5**, 4645 (2014).
25. Y. Hamamura *et al.*, *Nat. Commun.* **5**, 4722 (2014).
26. T. Dresselhaus, S. Sprunck, G. M. Wessel, *Curr. Biol.* **26**, R125–R139 (2016).
27. M. Schiott *et al.*, *Proc. Natl. Acad. Sci. U.S.A.* **101**, 9502–9507 (2004).
28. R. Völz, J. Heydlauf, D. Ripper, L. von Lyncker, R. Groß-Hardt, *Dev. Cell* **25**, 310–316 (2013).
29. D. Maruyama *et al.*, *Cell* **161**, 907–918 (2015).
30. X. Yu *et al.*, *Nature* **592**, 433–437 (2021).
31. C. Liu *et al.*, *Science* **372**, 171–175 (2021).
32. L. Zhang *et al.*, *Curr. Biol.* **31**, 3004–3016.e4 (2021).

ACKNOWLEDGMENTS

We thank D. Ye for providing *fer-4* and *myb97 myb101 myb120* mutant seeds; L. Smith for sharing *anj*, *herk1*, *anj herk1*, and *fer anj herk1* mutant seeds; J. F. Harper for providing *aca9* mutant seeds; and C. Li and Q. Duan for sharing *fer+/-* mutant seeds. **Funding:** L.-J.Q. was funded by the National Natural Science Foundation of China (grant nos. 31991202, 31830004, 31620103903, and 31621001), S.Z. was supported by the Young Elite Scientists Sponsorship Program by the China Association of Science and Technology (2019QNRC001), Z.G. was supported by a NSFC Young Scientists Fund (31900161), A.Y.C. was funded by the US Natural Science Foundation (IOS-1645854, MCB-1715764, and MCB-0955910), J.D. was funded by the National Institute of Health (RO1GM109080), and T.D. was supported by the German Research Foundation DFG (SFB924). **Author contributions:** S.Z. and L.-J.Q. conceived the project, and L.-J.Q. and H.G. supervised the project. S.Z., LiLi, Z.W., Z.G., and T.L. performed molecular cloning and CRISPR-Cas9-mediated mutant generation. S.Z., LiLi, and Z.W. performed phenotype observation and statistical analysis. LiLi and Z.W. analyzed the GUS activity with the help of Z.S., LuLi, and L.Z. S.Z., Z.G., and Y.S. performed RNA-seq analysis. Z.G., Q.L., and J.W. performed protein expression, protein purification, and all the protein-protein interaction assays with the help of H.Z., Y.W., and LuLa. A.B. and T.D. conducted receptor reporter localization assays. S.Z., J.D., H.-M.W., A.Y.C., T.D., and L.-J.Q. drafted the manuscript. All authors contributed to data analysis and manuscript preparation. **Competing interests:** The authors declare no competing interests. **Data and materials availability:** All data are available in the main text or the supplementary materials.

SUPPLEMENTARY MATERIALS

science.org/doi/10.1126/science.abl4683
Materials and Methods
Figs. S1 to S12
Tables S1 to S3
References (33–47)
MDAR Reproducibility Checklist

[View/request a protocol for this paper from Bio-protocol.](#)

15 July 2021; accepted 30 November 2021
10.1126/science.abl4683

RALF peptide signaling controls the polytubey block in *Arabidopsis*

Sheng ZhongLing LiZhijuan WangZengxiang GeQiyun LiAndrea BleckmannJizong WangZihan SongYihao ShiTianxu LiuLuhan LiHuabin ZhouYanyan WangLi ZhangHen-Ming WuLuhua LaiHongya GuJuan DongAlice Y. CheungThomas DresselhausLi-Jia Qu

Science, 375 (6578), • DOI: 10.1126/science.abl4683

Block to polyspermy

The next generation needs enough, but not too many, nuclear genomes. Zhong *et al.* show how the small mustard plant *Arabidopsis* both blocks polyspermy and also adds second-chance insurance when the first fertilization effort goes awry. Signals from the synergid cells in the female gametophyte invite a nearby pollen tube, which secretes peptides to block other pollen tubes from tagging along. The blockade persists as the pollen tube grows to its target. If the pollen tube successfully releases its pair of sperm (plants have a dual fertilization system), the pollen tube's signaling system fades to silence. If the female gametophyte successfully receives the sperm nuclei, invitational signals from the synergid cells also fade to silence. If, however, fertilization fails, the persistent signal from the synergid cells continues to attract pollen tubes and, because pollen tube rupture silenced the first pollen tube's block to polytuby, secondary pollen tubes are able to give another try at fertilization. —PJH

View the article online

<https://www.science.org/doi/10.1126/science.abl4683>

Permissions

<https://www.science.org/help/reprints-and-permissions>

Use of this article is subject to the [Terms of service](#)

Science (ISSN) is published by the American Association for the Advancement of Science. 1200 New York Avenue NW, Washington, DC 20005. The title *Science* is a registered trademark of AAAS.

Copyright © 2022 The Authors, some rights reserved; exclusive licensee American Association for the Advancement of Science. No claim to original U.S. Government Works